ELSEVIER

Journal of Physics and Chemistry of Solids 62 (2001) 2215–2221

JOURNAL OF PHYSICS AND CHEMISTRY OF SOLIDS

www.elsevier.com/locate/jpcs

The spectral momentum density of aluminum measured by electron momentum spectroscopy

M. Vos*, A.S. Kheifets, E. Weigold

Atomic and Molecular Physics Laboratories, Research School of Physical Sciences and Engineering, The Australian National University, Canberra ACT 0200, Australia

Abstract

Electron momentum spectroscopy is a tool ideally suited for the study of energy-resolved momentum densities. Here we present new data from a high-energy EMS experiment using 50 keV incoming and 25 keV outgoing electrons. Both the measured energy distributions and the measured momentum distributions are affected by multiple scattering. However, after correcting for these effects, neither distribution can be fully understood using electronic structure calculations that take electron–electron correlation into account only on a mean-field level.

1. Introduction

Of the many probes that are used in solid state physics only a few access properties that are directly related to the electron wave function. The momentum space wave function can be probed using high-momentum-transfer scattering experiments when the impulse approximation is valid. If one measures only the scattered particle this technique is referred to as Compton scattering (for photon scattering see, for example, Ref. [1], for electron scattering see, for example, Ref. [2]). In these experiments only a projection of the momentum density is resolved. The full momentum density can be resolved if one measures in coincidence the ejected electron as well. This technique is currently under development for photon scattering [3,4] and is referred to as $(\gamma,e\gamma)$ spectroscopy or (X,eX) spectroscopy. For electron scattering it is possible to resolve the separation energy of the ejected electron as well, and this technique is known as (e,2e) spectroscopy or Electron Momentum Spectroscopy (EMS) [5]. Initially the main success of this technique was in atomic and molecular physics, using gas-phase targets. For solids extremely thin targets and high electron energies are required to keep multiple scattering at a low level. Using the Flinders University spectrometer [6] semi-quantitative information was obtained from solids [7] and the importance of multiple scattering effects [8] became evident. Based on the experience with the Flinders spectrometer a new spectrometer was designed at the Australian National University [9] using 50 keV incoming and 25 keV outgoing electrons. Here we describe one of the first experiments of this spectrometer, estimate the effects of multiple scattering and compare the results with a theory that takes electron–electron interaction into account in an average way (Full Potential Linear-Muffin-Tin-Orbital calculation based on the local-density approximation of density-functional theory [10]). It is demonstrated that this average treatment of electron correlation effects is not sufficient to describe the current results.

2. Experimental details

The spectrometer is sketched in Fig. 1. It is described extensively in [9]. In brief, 25 keV electrons are emitted from the electron gun. The sample (and surrounding region) is at at +25 keV, so electrons with an energy of 50 keV impinge on the target. We try to measure (e,2e) events with maximum energy transfer. So the two detectors are tuned to detect 25 keV electrons. Each detector measures simultaneously a range of energies and (azimuthal) angles of the emerging electrons. These detectors are positioned at a polar angle of 44.3° corresponding to the Bethe ridge condition, i.e. at angles where we expect coincidences if we scatter from a stationary particle. (The relative angles between the emerging electrons is slightly less than 90° due to relativistic effects.) If all three trajectories are in the same

* Corresponding author. Tel.: +61-2-6249-4985; fax: +61-6249-2452.

E-mail address: vos107@rsphysse.anu.edu.au (M. Vos).

0022-3697/01/$ - see front matter
PII: S0022-3697(01)00180-9

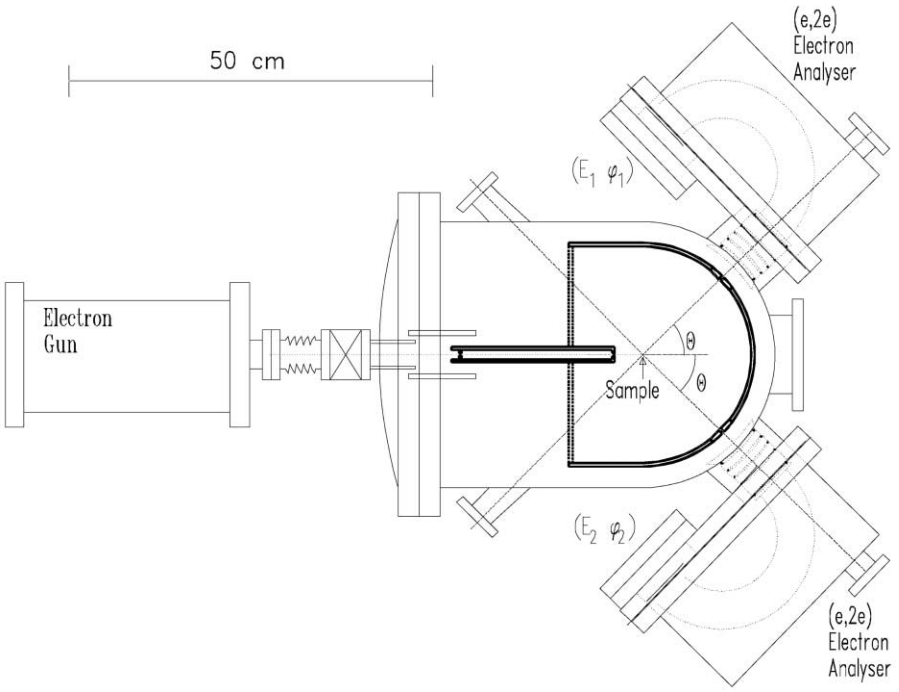

Fig. 1. A schematic representation of the spectrometer as described in the text.

plane we scattered indeed from a stationary particle. If the third electron has a momentum component perpendicular to the plane defined by the incoming and the other outgoing electron, we scattered from an electron with momentum equal to this perpendicular component.

Under the high momentum transfer conditions, where the plane-wave impulse approximation is well justified, we can infer the binding energy and momentum of the struck electron by comparing the energy and momentum of the incoming and both outgoing electrons. For an interacting electron gas, where we cannot identify the binding energy and momentum of a single electron, the probability that a certain energy-momentum difference occurs between the incident and two outgoing electrons is proportional to the spectral function.

Aluminum was evaporated on a thin ($\simeq$ 35 Å) free standing carbon substrate covering a number of 0.8 mm diameter holes. The thickness was monitored by a crystal thickness monitor and judged to be close to 100 Å. The film was sputtered from the carbon side using 800 eV Ar^+ ions, until some of the films broke. Thus, assuming that at this time the carbon film was completely removed, we have now a freestanding polycrystalline aluminum film. Subsequently the film was transferred to the spectrometer and measured. This was all done in three interconnected vacuum chambers without exposing the sample to air. Pressure in the evaporation and sputtering chamber was in the 10^{-9} torr range and in the measurement chamber the pressure was 4×10^{-10} torr during the experiment. From experiments at Flinders under comparable conditions [11] we know that the thickness of oxide acquired under these conditions is only about 25% of the saturation thickness of the oxygen layer after prolonged exposure to oxygen $\simeq$10 Å [4]. The current spectrometer measures the whole thickness of the film with comparable efficiency and the contribution of the oxide layer should thus be of the order of 5%. No clear indication of either carbon (indicating that this layer was removed by the sputtering) or aluminum oxide were observed in the EMS data.

3. Results and discussion

The measurement lasted for 2 days. The beam current was 800 nA and the coincidence count rate approximately 1 Hz. The results are shown in Fig. 2 (left panel). There are three clear features, a parabola starting at $\simeq$11 eV binding energy and extending to the Fermi level, corresponding to the quasi-particle peaks of aluminum, a repeat of this feature at 15 eV larger binding energy and a weak non-dispersive feature around 74 eV. This last feature corresponds to the Al 2p level. However the measured intensity does not drop to zero, even at largest binding energies.

This is a consequence of inelastic multiple scattering. For a discussion of multiple scattering of electrons in solids see Ref. [12]. Along the incoming and outgoing trajectories additional scattering events can occur (mainly plasmon excitation) which shift the inferred binding energy (i.e. the difference in kinetic energy of the incoming electron

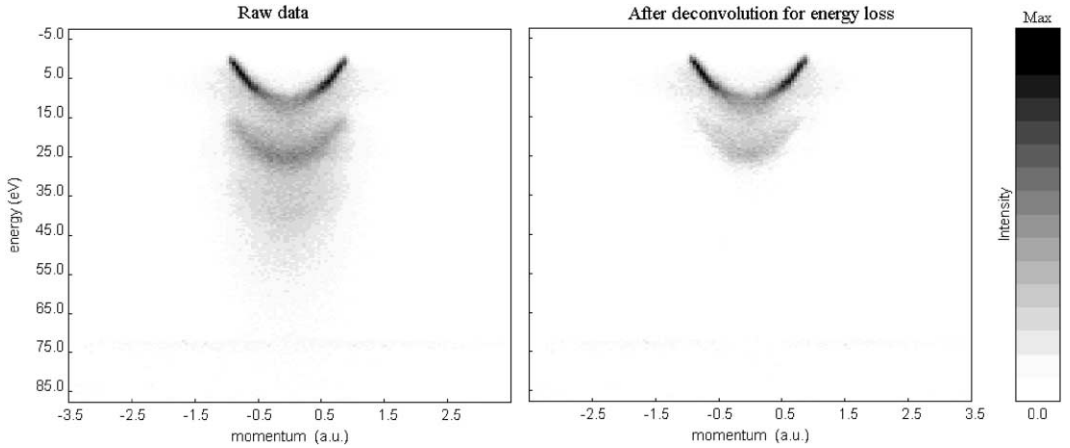

Fig. 2. The measured spectral momentum density of a thin aluminum film. The left panel shows the raw data, the right panel is corrected for inelastic multiple scattering as described in the text.

and the sum of the kinetic energy of both outgoing electrons) to larger values. The inelastic mean free path for 25 and 50 keV electrons is approximately 280 and 520 Å, respectively.

Similarly elastic multiple scattering (deflection of the incoming and outgoing electrons from the nuclei) can cause the wrong momentum to be attributed to the (e,2e) event. The elastic mean free path of 25 and 50 keV electrons in aluminum are estimated to be 240 and 480 Å, respectively.

First we will try to estimate the effect of inelastic scattering. This is done by measuring an energy loss spectrum using one of the two (e,2e) electron analysers. For this purpose the energy of the incoming electrons is reduced from 50 to 25 keV and we measure an elastic peak in the electron analyser (these electrons have been elastically scattered over 44.3°, the angle at which the analyser is positioned relative to the incoming beam) followed by a loss distribution due to inelastic scattering (in addition to the elastic scattering over 44.3°). This loss distribution is shown in Fig. 3. The ratio of the area of the energy loss part of this distribution to the area of the elastic peak is proportional to the sample thickness. However in the (e,2e) event we have a somewhat different situation with an incoming electron (50 keV) and two (25 keV) outgoing electrons and we can, hence, have a different ratio of event with and without inelastic multiple scattering. The path length of electrons in the (e,2e) events (corrected for the larger inelastic mean free path of the 50 keV electron

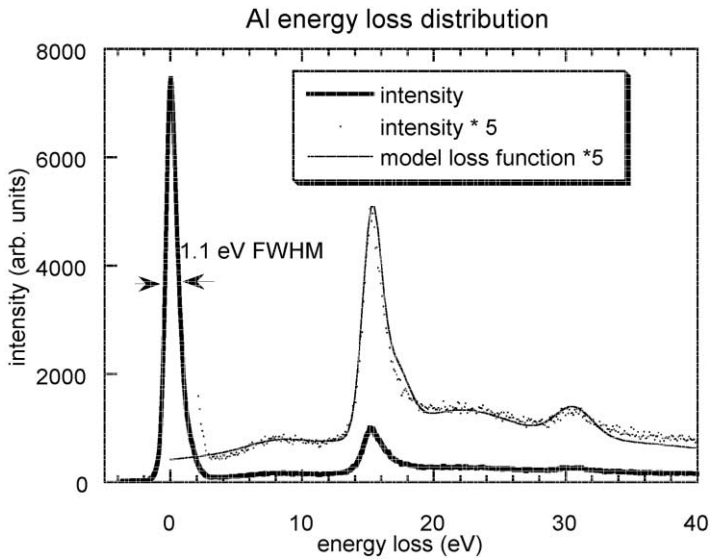

Fig. 3. The measured energy loss distribution of 25 keV electrons transmitted through the aluminum film. The measured loss distribution was used to correct the EMS data for inelastic multiple scattering.

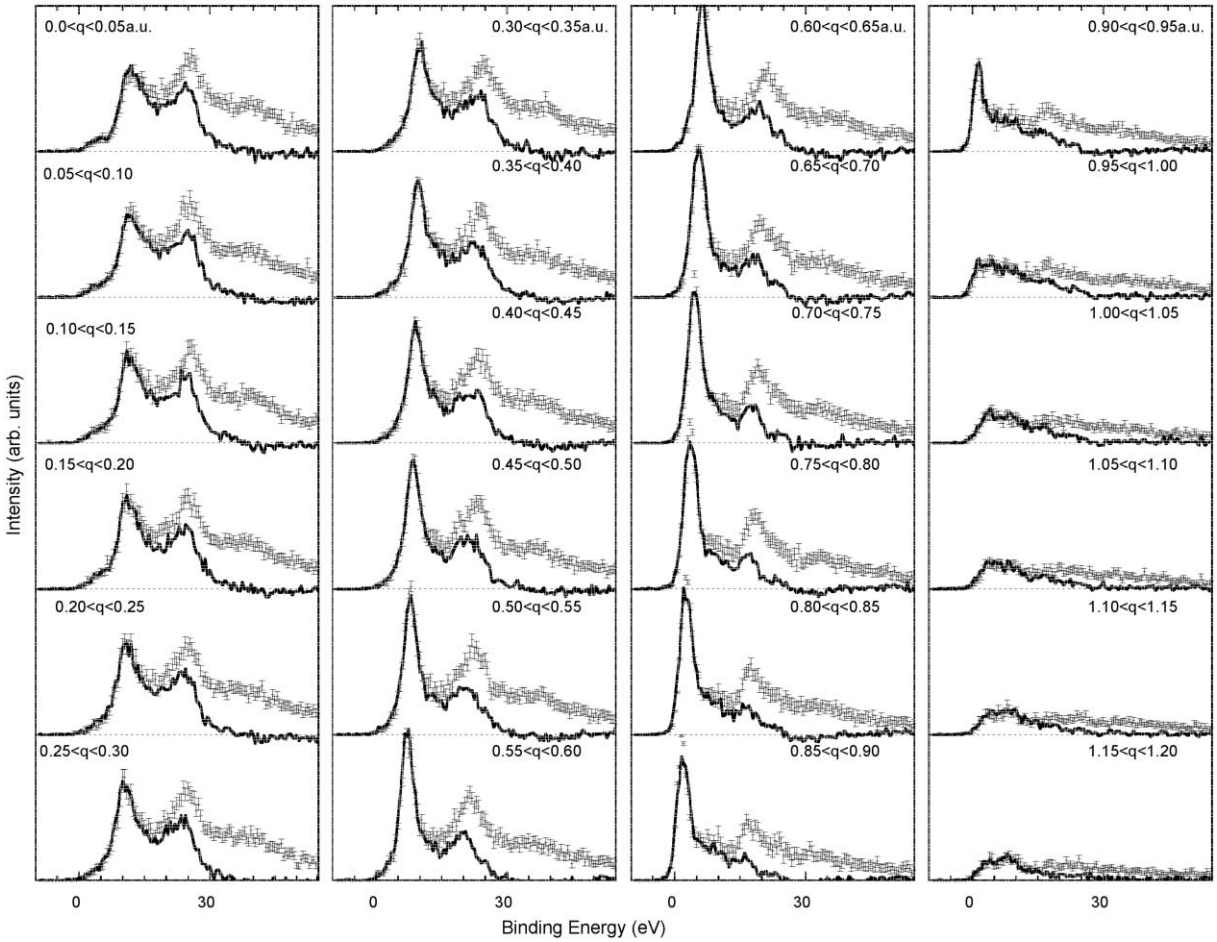

Fig. 4. The measured spectra for different momentum intervals as indicated (in a.u.). The deconvoluted spectra (full line) and the raw data (error bars) are shown. The intensity of the deconvoluted spectra does not drop to zero at binding energies immediately above the quasi-particle but only at about 20 eV above these peaks due to electron–electron interactions.

compared to that of 25 keV electrons) differs from that of the elastic scattering experiment and depends on the depth at which the (e,2e) event took place. For an (e,2e) event in the centre of the film the effective thickness of the film is $\simeq$1.4 times that of the elastic experiment, a value we take to be representative for the whole experiment. Using a fit to the measured energy loss distribution and the measured ratio of the energy loss area to elastic peak area (multiplied by 1.4) we can subtract the (e,2e) events with additional inelastic scattering [13]. The result is shown in the right panel of Fig. 2. Now there is a large region without noticeable intensity in between the valence band and the core level. Notice the minimum in intensity of the core electron contribution near zero momentum, as expected for a 2p level.

A more quantitative impression of the valence band part of the measurement is obtained from plotting the actual spectra as is done in Fig. 4. The error bars are the raw data, the full line is after correction for inelastic scattering as described above. After deconvolution the intensity straggles zero at the high binding energy side for all momentum intervals. An identical deconvolution procedure, completely constrained by experimental data, works for various carbon films [14] as well as for copper and gold [15], which indicates that it captures the physics of the inelastic contribution quite well. The quasi-particle peak disperses from 11 eV binding energy (relative to the Fermi level) at zero momentum to 0 eV binding energy near 0.9 a.u. Near zero momentum the quasi-particle peak is rather broad due to life-time broadening ($\simeq$4 eV, exceeding the experimental resolution of 2 eV), and becomes narrower at larger momentum. Near k_f the width is completely determined by the experimental resolution. The second (satellite) peak at higher binding energy is separated by the quasi-particle peak by about a plasmon energy. In the raw data it is partly due to inelastic multiple scattering as it is reduced significantly by the deconvolution, however it still remains strong after removal of the inelastic multiple scattering effects.

Indeed it is in this energy range that one expects additional intensity due to electron–electron interaction. The medium screens the electron–electron interaction due to density fluctuations, similar to those in plasmons. Removal of an electron by an impulsive collision may therefore result in the creation of a plasmon. Therefore the spectral function will show two peaks at a given momentum: one corresponding to the quasi-particle binding energy and one shifted by the plasmon energy to larger binding energies. Many-body calculations indicate about 30% of the intensity should be in this range, see, for example, Refs. [16–19]. In the photoemission literature it is referred to as 'intrinsic plasmons' [20]. The shape of this satellite feature is broader than that of the plasmon measured in the loss experiment, having non-negligible intensity everywhere from the quasi-particle peak up to about 20 eV below this peak. A similar conclusion was reached using the Flinders University data, although this data was interpreted rather differently [21]. In that interpretation the EMS data were compared with Monte Carlo simulations using a spectral function, based on the cumulant expansion technique [22], as an input.

As a caveat we want to point out that the carbon σ-band has intensity at similar momentum-energy combinations as the aluminum satellite structure [14]. However the observed rapid decay near 0.95 a.u. is *not* typical for carbon. Thus if any carbon remained after removal by sputtering its intensity can only correspond to a very small fraction of the observed satellite structure.

Above 0.95 a.u. the intensity of the quasi-particle peak should drop to zero, as it reaches the Fermi level near 0.93 a.u. Calculations indicate that the intrinsic plasmon satellite should persist up to higher momenta [16] and thus cause a tail extending to higher momenta in the momentum density distribution. Deriving this tail from our measurements is complicated by elastic scattering events. Elastic scattering generally changes the momenta of electrons by the order of 1 a.u. The momentum distribution derived from (e,2e) events with additional elastic multiple scattering is thus redistributed over a fairly broad range of momenta.

This is illustrated by the measured momentum distribution derived from electrons near the Fermi level (E_f). As the spectrometer measures negative as well as positive momenta we measure a distribution that is (except for statistical fluctuations) symmetric relative to zero momentum. From the density of electrons in aluminum we expect the maximum momentum value of occupied quasi-particle peak to be at 0.93 a.u. Indeed we see peaks close to this value (0.88 a.u.). The difference between these two values is easily explained by the fact that due to our finite energy resolution states slightly away from the Fermi level also contribute to the measured intensity and thus give a lower mean momentum for the peak.

As there are no states occupied above E_f no (e,2e) events contaminated with inelastic scattering can contribute at E_f. Inelastic multiple scattering can only remove events from this momentum distribution, and thus reduce its overall intensity. The shape of the momentum distribution at the Fermi level is affected only by elastic multiple scattering. In Fig. 5, we compare the measured intensity with those obtained from Monte Carlo simulations (taking into account both elastic and inelastic multiple scattering) [8] as a function of film thickness. These simulations use as input data the density obtained from a band structure calculation, i.e. without the intrinsic plasmon type satellite. The observed intensity has sharp peaks with some broader feet. The simulations were done assuming a momentum resolution of 0.05 a.u. The simulation of 100 Å thick film reproduces the right background intensity at zero momentum, whereas the intensity at high momentum ($\simeq$2 a.u.) seems to be reproduced by the 200 Å simulation.

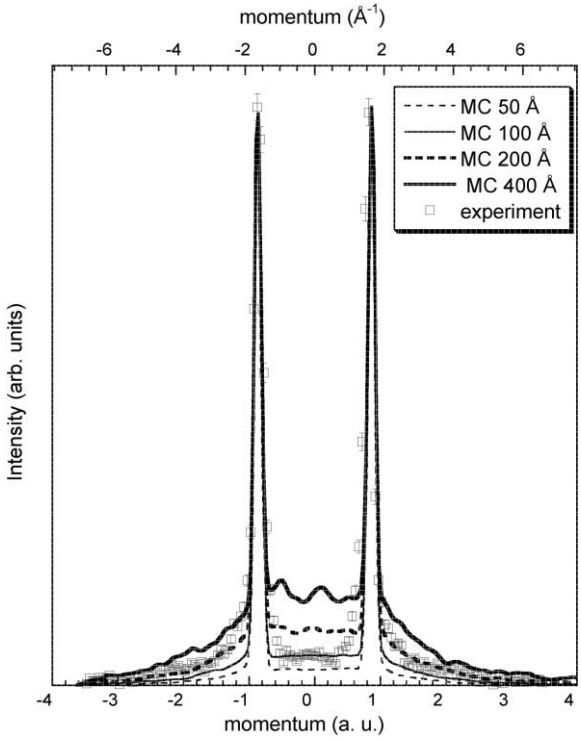

Fig. 5. The simulated momentum density near the Fermi level for different thicknesses of aluminum compared to the measured one. The measured and simulated distributions are all normalised to equal height of the quasi-particle peak of the spectral function. The amount of multiple scattering increases with film thickness.

Simultaneously we can derive the total momentum density from these simulations. In Fig. 6, we compare the simulated intensity between 0 and 55 eV binding energy with the simulated intensity between 0 and 2 eV. With increasing film thickness a larger and larger fraction of the (e,2e) events have experienced inelastic multiple scattering. Thus the intensity near the Fermi level, relative to the total intensity, will decrease with increasing sample thickness. Also larger thicknesses will increase the broad (in momentum) pedestal due to (e,2e) events with elastic multiple

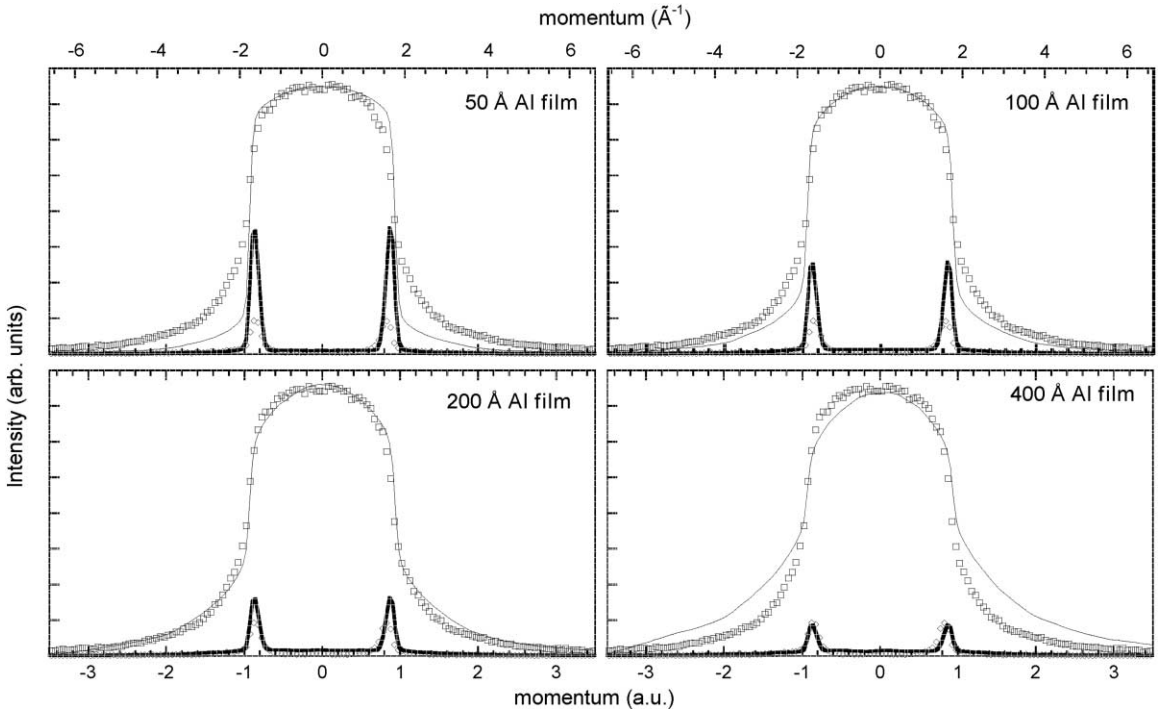

Fig. 6. The simulated intensity distribution, integrated from 0 to 55 eV binding energy for aluminum films of different thickness (thin solid lines). Also plotted is the simulated intensity in the 2 eV window just below the Fermi level (thick solid line). The simulations are compared with the experiment (squares and diamonds, respectively).

scattering i.e. the break near k_f becomes less and less pronounced. Indeed all of these trends are observed in the simulations. In this figure we show the measured distributions integrated over the same energy windows as well, normalised to the same height as the simulation of the total distribution. None of the simulations reproduce all the experimental data. Due to the electron–electron correlation, *not* contained in the input theory used in the simulation, a significant fraction of the intensity is shifted away from the Fermi level (expected to be near 30%) by about a plasmon energy. Thus we expect the theory to overestimate the intensity near E_f relative to the total intensity. This is indeed the case for all the simulations except the 400 Å one. However there the integrated distribution is clearly too broad. Thus the film thickness is less than 400 Å (as we concluded from the *shape* of the distribution near E_f as well). The 50 Å simulation shows a large discrepancy between the measured and simulated intensity near E_f so again we conclude that the film is thicker than 50 Å. The 200 Å simulation shows about a 30% excess intensity near E_f and the total momentum distribution fits the experiment rather well. This is surprising as the high-momentum tail in the momentum distribution is not contained in the theory. The 100 Å simulation is indeed somewhat too narrow, however simulated intensity at E_f is close to a factor of 2 larger than the observed, not all of which can be due to removal of intensity by the many-body effects (satellite structure).

4. Conclusions

In this paper we reported a preliminary analysis of the new high energy (e,2e) experiment on an aluminum film. The energy spectra show intensity away from the quasi-particle peak, much more than expected due to inelastic multiple scattering. This excess intensity can only result from electron–electron correlations. Similarly the width of the quasi-particle peak depends on the momentum and it is at its broadest at the bottom of the quasi-particle band ($\mathbf{q} = 0$). It is approximately 4 eV wide, indicating a short lifetime. The momentum distributions turn out to be a critical test as well. Using state-of-the-art band structure calculations it is not possible to describe the total (energy-integrated) momentum density and the momentum density near the Fermi level simultaneously. Currently we are in the process of performing a full many-body calculation over the whole momentum range on a fine momentum grid. This study will give a better description of the experiment, as it will contain intrinsic satellite contributions and, hence, should also reproduce the high-momentum tail of the momentum distribution. A definitive comparison may,

however, require the use of even thinner films, so that the multiple scattering contributions are less important in the comparison with theory.

References

[1] M. Cooper, Compton scattering and electron momentum determinations, Rep. Prog. Phys. 48 (1985) 415.

[2] T.S.B.G. Williams, R. Egerton, Electron Compton scattering from solids, Proc. R. Soc. A 393 (1984) 409.

[3] M. Itou, S. Kishimoto, H. Kawata, M. Ozaki, H. Sakurai, F. Itoh, Three-dimensional electron momentum density of graphite by (x,ex) spectroscopy with a time of flight electron energy spectrometer, J. Phys. Soc. Jpn. 68 (1999) 515.

[4] C. Metz, T. Tschentscher, P. Suotti, A. Kheifets, D. Lun, T. Sattler, J. Schneider, F. Bell, Three dimensional electron momentum density of aluminum by (γ,eγ) spectroscopy, Phys. Rev. B 59 (1999) 10512.

[5] I. McCarthy, E. Weigold, Electron momentum spectroscopy of atoms and molecules, Rep. Prog. Phys. 54 (1991) 789.

[6] P. Storer, R. Caprari, S. Clark, M. Vos, E. Weigold, Condensed matter electron momentum spectrometer with parallel detection in energy and momentum, Rev. Sci. Instrum. 65 (1994) 2214.

[7] M. Vos, I. McCarthy, Observing electron motion in solids, Rev. Mod. Phys. 67 (1995) 713.

[8] M. Vos, M. Bottema, Monte Carlo simulations of (e,2e) experiments in solids, Phys. Rev. B 54 (1996) 5946.

[9] M. Vos, G. Cornish, E. Weigold, A high-energy (e,2e) spectrometer for the study of the spectral momentum density of materials, Rev. Sci. Instrum. 71 (2000) 3831.

[10] A. Kheifets, D. Lun, S.Y. Savrasov, Full-potential linear-muffin-tin-orbital calculation of electron momentum densities, J. Phys.: Condens. Matter 11 (1999) 6779.

[11] S. Canney, M. Vos, A. Kheifets, X. Guo, I. McCarthy, E. Weigold, Electron momentum spectroscopy studies of the oxidation of aluminium, Surf. Sci. 382 (1997) 241.

[12] R. Shimizu, Z.-J. Ding, Monte Carlo modelling of electron–solid interactions, Rep. Prog. Phys. 55 (1992) 487.

[13] R. Jones, A. Ritter, Analysis of multiple scattering for (e,2e) experiments on thin film, J. Electron. Spectrosc. Relat. Phenom. 40 (1986) 285.

[14] M. Vos, A. Kheifets, E. Weigold, Clear evidence of electron correlation effects in the spectral momentum density of graphite, Phys. Rev. B 63 (2001) 033108.

[15] M. Vos, A.S. Kheifets, E. Weigold, unpublished.

[16] B. Lundqvist, Single-particle spectrum of a degenerate electron gas, Phys. Kondens. Mater. 6 (1968) 193.

[17] R. Godby, Unoccupied Electronic States, Springer-Verlag, Berlin, 1991, p. 53 Ch. Exchange and correlation in solids.

[18] B. Holm, U. von Barth, Fully self-consistent gw self-energy of an electron gas, Phys. Rev. B 57 (1998) 2108.

[19] L. Hedin, On correlation effects in electron spectroscopies and the GW approximation, J. Phys.: Condens. Matter 11 (1999) R489.

[20] P. Steiner, H. Höchst, S. Hüfner, Photoemission in Solids, vol. 2, Springer-Verlag, Berlin, 1978, p. 349 Ch. Simple Metals.

[21] M. Vos, A. Kheifets, E. Weigold, S. Canney, B. Holm, F. Aryasetiawan, K. Karlsson, Determination of the energy-momentum densities of aluminium by electron momentum spectroscopy, J. Phys.: Condens. Matter 11 (1999) 3645.

[22] F. Aryasetiawan, O. Gunnarsson, The GW method, Rep. Prog. Phys. 61 (1998) 237.